Dynamic Response of the Coupled Vehicle-Floating Slab Track System using Finite Element Method

Morteza Esmaeili [1], Saeed Mohammadzadeh [2], Mohammad Mehrali [3]

Received:26.02.2015 Accepted:28.02.2016

Abstract

In present study, a mathematical model of the vehicle–floating slab track (FST) interaction is established to investigate the coupled behaviour of vehicle–track system. The FST is modelled as the double Euler -Bernoulli beam including the rail and slab. The railway vehicle is simplified as a multi-rigid-body model. The wheel–rail interface is treated using a nonlinear Hertzian contact model, coupling the mathematical equations of the vehicle–FST systems. The dynamic interaction of the entire system is numerically studied in time domain, employing Newmark's integration method. The numerical model of the present research is validated using benchmark model reported in the literature. Finally using the developed numerical tool many sensitivity analyses were performed on various important parameters affecting on dynamic behaviour of slab track, such as slab thickness, axle load and the track bed stiffness and consequently the deflection and bending moment of rail and slab were assessed. Slab thickness has more effect on slab than rail dynamic behaviour.

Keywords: Vehicle-FST Interaction, Double Euler Bernoulli beam, dynamic response

* Corresponding author Email: m_esmaeili@iust.ac.ir

1. Associate Professor, School of Railway Engineering, Iran University of Science and Technology, Tehran, Iran
2. Assistant Professor, School of Railway Engineering, Iran University of Science and Technology, Tehran, Iran
3. PhD. Candidate, School of Railway Engineering, Iran University of Science and Technology, Tehran, Iran

1. Introduction

In the recent decades, slab track system comparing to those of traditional ballasted track, due to the superior structural capacity, low life cycle costs (LLC) and low volume of track maintenance activities has gained more attraction by railway track designers and railway owners as well. Referring to available literature it can be understood that the most accurate analytical models deal with evaluation of dynamic response of the mentioned system as infinite double beams or infinite beam rested on infinite slab under moving loads or moving masses. In this regard and as a practical case [Ding et al. 2011] carried out a laboratory test in order to obtain the characteristics of low frequency vibrations and performance of a FST. [Hussein and Hunt, 2006] and [Hussein and Hunt, 2009] studied the response of FST including continuous and discontinuous slabs to an oscillating moving load. In another study, [Gupta and Degrande, 2009] investigated the periodicity of the track and the tunnel–soil system using the Floquet transform to formulate the problem in the frequency– wavenumber domain. A coupled periodic finite element–boundary element method was used to model the tunnel–soil system, while a periodic finite element model (FEM) or an analytical approach was used to model the track. [Jun, Dan and Qing, 2009] studied the spatial vibration equation of the high-speed train and slab track system on the basis of the principle of total potential energy with stationary value in elastic system dynamics. [Yen and Lee, 2007] investigated the parameter identification of slab track using 3D FEM. Their aim was to idealize theoretical solutions for a continuously and elastically supported beam and two continuous beams on elastic foundations subjected to a concentrated load. [Li and Wu, 2007] looked into the vibration isolation performance of different lengths FST under a harmonic moving load. [Steenbergen, Metrikine and Esveld, 2007] employed a classical model of a beam on elastic half-space subjected to a moving load in order to provide the required stiffness of slab track system. In another study, [Lombaert et al, 2006] studied the effectiveness of the FST using a track-soil coupled model for controlling of the ground-borne vibration generated by railway traffic. In addition to the theoretical studies, experimental investigations on the FST systems have been accomplished by using test rig [Cox et al. 2006] or in situ [Saurenmann and Phillips, 2006]. [Mohammadzadeh, Esmaeili and Mehrali, 2013] assessed the response of a double beam as a slab track system considering random stiffness for foundation of track. In continue, [Mehrali et al. 2014] simulated a coupled vehicle - slab track by FEM in the case of random stiffness of the rail foundation.

An extensive literature cab found regarding to simulation of finite double beams with in between resilient layer. [Abu-Hilal, 2006] investigated the dynamic response of a double-beam system traversed by a constant moving load. In their work two parallel simply supported prismatic beams were considered which they were continuously connected by a viscoelastic layer. [Xiaobin et al. 2014] presented an exact stiffness method to determine the natural frequencies and mode shapes of the axially loaded double-beam systems.

[Kuo et al. 2008] developed an analytical model to investigate the vibration behaviour of slab track under loading of a simple 1/8 car model. [Yuan, Zhu and Wu, 2009] employed an analytical dynamic model to assess vibration characteristics and effectiveness of FST. All above mentioned researches have studied the behaviour of slab track using analytical methods ignoring the vehicle - slab interaction effect.

In the current study, coupled vehicle- double beam dynamic interaction is investigated by using FEM to represents the dynamic response of FST system in practice. In the developed model, the track superstructure including the rails and FST are considered as two parallel Euler–Bernoulli beams. The upper beam accounts for the rail and the lower one accounts for the concrete slab. Both beams are connected together via a series of springs and dashpots to represent the stiffness and damping of rail pads. On the other hand, the lower beam (slab) is rested on a visco-elastic bearing layer by means of a series of parallel springs and dashpots. The vehicle is a whole rolling stock with two layers of spring and damping system in which vertical and rolling motion for vehicle and bogie are involved. Coupling the vehicle system and railway track is realized through interaction forces between the wheels and the rail by using nonlinear Hertz contact theory. In continue, utilizing the developed numerical tool many sensitivity analyses are carried out on the parameters

which remarkably influence on the slab track dynamic response such as slab thickness, slab bearing stiffness and axle load. Consequently the rail and slab deflection and bending moment are achieved.

2. FEM Model Configuration

To study the coupled integration of the train–track system, various mathematical models were established. In the present work, the dynamic model of vehicle and track is extended. The general configuration of developed FE coupled model including FST and vehicle is described and in the next section the solution procedure of the assembled systems of governing equations is explained.

2.1 FST Subsystem

The components of the FST system as doubled beam, including the rail and slab is shown in Figure 1. As illustrated, a series of two node beam elements with two degree of freedom in each node, one sets for vertical deflection and another assigned to the rotation are adopted for both rail and slab.

Rail pads are represented by a layer of springs with stiffness k_1 and a viscous damping factor c_1 which connect the rail to slab. Moreover, slab bearing is represented by a layer of springs with stiffness k_2 and a viscous damping factor c_2. The equation of motion for the slab track is:

$$\begin{bmatrix} M_{Rail} & 0 \\ 0 & M_{Slab} \end{bmatrix} \begin{Bmatrix} \ddot{u}_{r_t} \\ \ddot{u}_{s_t} \end{Bmatrix} + \begin{bmatrix} C_{Rail} & 0 \\ 0 & C_{Slab} \end{bmatrix} \begin{Bmatrix} \dot{u}_{r_t} \\ \dot{u}_{s_t} \end{Bmatrix} + \begin{bmatrix} K_{Rail} & 0 \\ 0 & K_{Slab} \end{bmatrix} \begin{Bmatrix} u_{r_t} \\ u_{s_t} \end{Bmatrix} = \{F\}_t \quad (1)$$

In which index 't' refers to the whole track assembly. Where,, and are mass, damping and stiffness matrixes of the rail, respectively, , and are corresponding to acceleration, velocity and displacement vectors of the rail. , and are mass, damping and stiffness matrixes of slab,, and are the acceleration, velocity and displacement vectors of the slab, respectively. denotes the external load vector of the vehicle model.

Coupling of matrices for the track elements is performed by manipulating the interconnecting matrices, based on their common DOFs. In the present study a 50 meter long track is simulated and each element' length is considered to be 0.5 meter.

a. Vehicle Subsystem

The vehicle system consist of vehicle body mass and its moment of inertia, the two bogie masses and their moments of inertia, and mass/inertia of four wheel-sets. Each bogie frame is connected to wheel-sets through the primary suspension springs/dashpots (K_p/C_p) and to the car-body through the secondary suspension (K_s/C_s). The car body and two bogies each undergo vertical displacement and pitch rotation, but only vertical displacement is considered in the four wheel-sets. Thus, the vehicle is modelled as 10 degrees of freedom multi body system. The equation motion of vehicle are listed in Appendix.

The equation of motion for whole vehicle model is as follows:

$$[M_v]\ddot{U}_v(t) + [C_v]\dot{U}_v(t) + [K_v]U_v(t) = F_v \quad (2)$$

where , and are the mass, damping and stiffness matrices and , , and are the acceleration, velocity and displacement vectors of the vehicle model, respectively. These matrices are symmetric and obtained by assembling the corresponding matrix of all components within the concerned DOFs.

b. Wheel-Rail Interface Model

Various models are available to define the contact interface between the wheel and the rail. In addition to the conventional Hertzian elastic contact theory, more sophisticated models have developed in the literature, including longitudinal creepage, frictional behaviour and braking/traction forces, see for example [Kalker, 1991], [Zhao and Li, 2011], [Zhao, Li and Liu, 2012].

According to Eqs (1)-(2), the equation of motion for the coupled vehicle-slab track system can be written as

$$[M_v]\{\ddot{U}_v\} + [C_v]\{\dot{U}_v\} + [K_v]\{U_v\} = F_v(t) \quad (3)$$

where , and are the mass, damping and stiffness matrices of the coupled vehicle-FST system, respectively, , and are the acceleration, velocity and displacement vectors of the coupled vehicle-FST system, respectively and is the external load vector which is determined by the track irregularity.

Here, the vehicle and FST contact model is considered

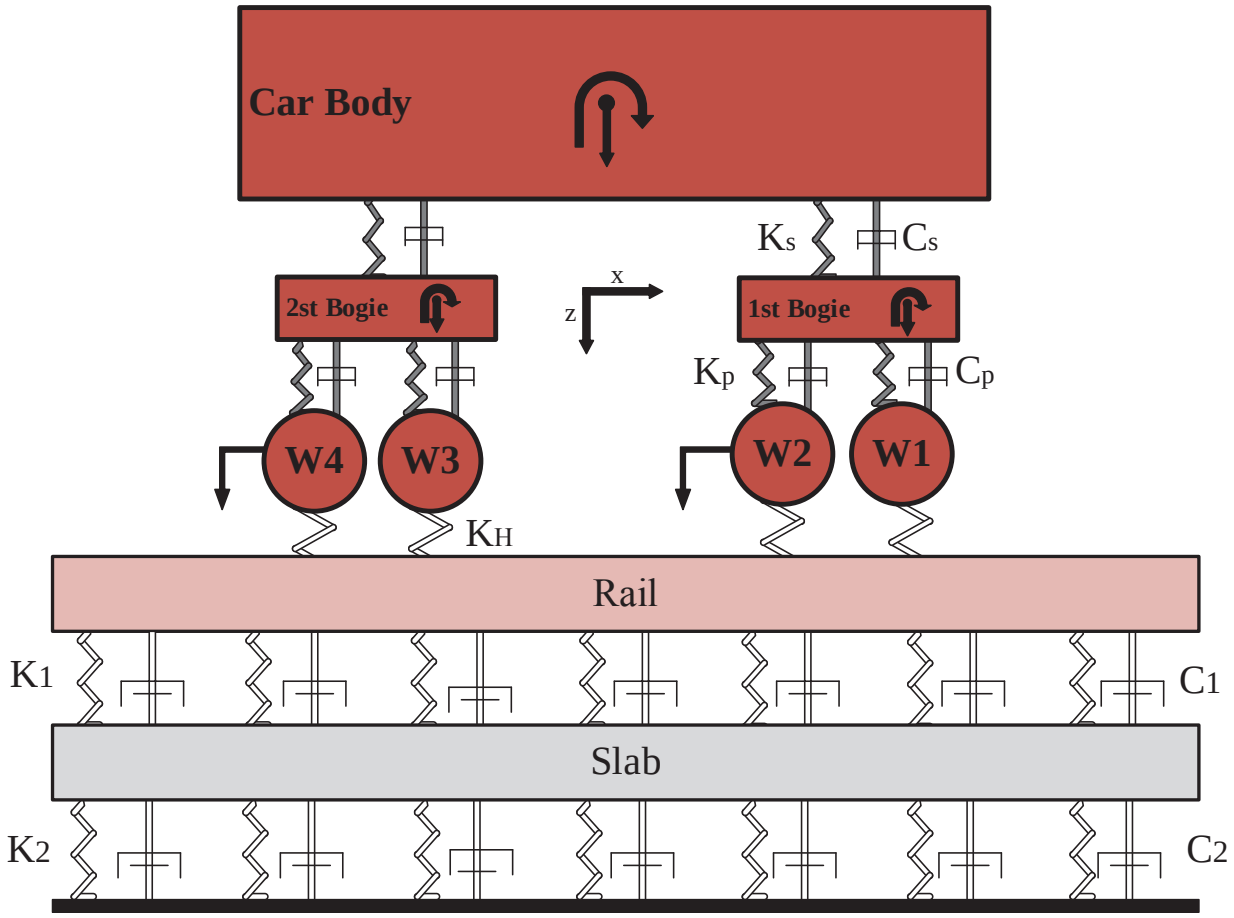

Figure 1. Model configuration of coupled vehicle - FST

to be non-linearized Hertzian wheel-rail model which is expressed as

$$f_w = C_H[U_w - U_r - U_{irr}]^{1.5}$$

$$f_{\dot{w}} = K_H[U_{\dot{w}} - U_r(U_j, t) - U_{irr}(U_j)]$$

$$K_H = C_H[U_w - U_r - U_{irr}] \quad (4)$$

$$f \quad U_w > U_r + U_{irr}(U)$$

$$K_H = 0$$

$$f \quad U_w > U_r + U_{irr}(U)$$

where refers to the irregularities of the rail surface.

In Eq. (3) the stiffness matrix is time - dependent and is determined by the contact location between wheel and rail. The stiffness matrix is updated in each time step and the time variant term of the stiffness matrix is transferred into the right side of the Eq. (3) for convenient calculation of the system response [Zakeri and Xia, 2008] , [Zhai et al. 2009].

The coupled vehicle-FST system is divided into two time-invariant subsystems including the vehicle and the FST.

The interaction between these subsystems is accomplished through the wheel-rail force. The responses of the vehicle and FST can be obtained independently using step-by-step numerical integration.

The assembling of whole system matrixes considering the vehicle and slab track components in matrix form can be presented as equation (5).

In the following system matrixes, [C], [B], [W] are car body, bogies and wheel-sets relevant matrixes, respectively.

The interaction between car body, bogies and wheel-sets are applied by [C/B], [B/W] and [W/R] matrixes.

$$\begin{bmatrix} [C] & [C/B] & 0 & 0 & 0 \\ [C/B] & [B] & [B/W] & 0 & 0 \\ 0 & [B/W] & [W] & [W/R] & 0 \\ 0 & 0 & [W/R] & [R] & [R/S] \\ 0 & 0 & 0 & [R/S] & [S] \end{bmatrix} \quad (5)$$

[R] and [S] are the rail and slab matrixes and these two elements are connected together via [R/S] matrix. Moreover, the interaction between rail and vehicle is established by [W/R] matrix.

3. Solution Method

In order to solve the final motion equation of the system the numerical time-integration method of Newmark-β [Ames, 1972] is employed. Using this numerical technique, responses of the track and vehicle elements are calculated in each time step as the vehicle moves along the track. Based on Newmark's method knowing the system response in time t, its response can be determined in time (t+dt) by:

$$\begin{aligned} &([K]+a_1[M]+a_2[C](U_{t+\Delta t}\} = F_{t+\Delta t} + \\ &+[M](a_1U_t + a_3\dot{U}_t + a_4\ddot{U}_t) + \\ &[C](a_2U_t + a_5\dot{U}_t + a_6\ddot{U}_t). \\ &\{\dot{U}_{t+\Delta t}\} = a_2(U_{t+\Delta t} - U_t) - a_5\dot{U}_t - a_6\ddot{U}_t \\ &\{\ddot{U}_{t+\Delta t}\} = a_1(U_{t+\Delta t} - U_t) - a_3\dot{U}_t - a_4\ddot{U}_t \end{aligned} \quad (6)$$

The values of a_1 to a_6 can be calculated by the following equations:

$$\begin{aligned} &a_1 = \frac{1}{\alpha dt^2},\ a_2 = \frac{\beta}{\alpha dt}, \\ &a_3 = \frac{1}{\alpha dt},\ a_4 = \frac{1}{2\alpha} - 1 \\ &a_5 = \frac{\beta}{\alpha} - 1,\quad a_6 = \frac{dt}{2}(\frac{\beta}{\alpha} - 2) \end{aligned} \quad (7)$$

Where α and β are parameters of Newmark's method. Considering the α=0.25 and β=0.5, the numerical stability of the solution is guaranteed [Mohammadzadeh, Ahadi, Keshavarzian, 2014]. A numerical code is developed in MATLAB for solving the dynamic interaction of the vehicle–track system using Newmark-β method. The general procedure of the numerical simulation in this study is presented in Figure2. Employing this numerical technique, the responses of the track and vehicle components were calculated in each time-step as the vehicle moves along the track. The motion of the wheel-sets was coincided with the motion of the rails, while the wheel-rail contact forces were considered in the calculations.

The contact forces between wheel and rail elements appeared in the numerical procedure while the wheels running at rail beam joints. Applying this procedure, the stiffness and damping matrices of the rail and wheel elements were gradually updated by manipulating the input matrices. The procedure of conducted numerical simulation is presented in Fig 2.

4. Numerical Results and Discussion

In current section firstly the validity of the developed model is investigated through comparison of the obtained results of FE model with existing analytical results. In continue some sensitivity analyses are preformed to show some considerable aspects in dynamic behaviour of slab track system.

4.1 Model Validation

The proposed model in current research is verified trough a comparative evaluation with the presented analytical and experimental results of [Hussein and Hunt, 2006].

As a numerical example vertical deflection of current model consist of infinite beam rested on a visco-elastic foundation under moving load with various speeds is compared with those have been obtained in the case of passing a non-harmonic moving load along an infinite beam with various speeds [Hussein and Hunt, 2006] for verification and validation purposes. The amplitude of the moving load is assumed to be unit (Figure 3).

Figure 4 gives the vertical rail displacement when the unit load is running in various speed from 0 to 450 m/s over the infinite double beam. Table 1 shows the percentage error of simulated model with the [Hussein and Hunt, 2006] work. It is illustrated that the maximum error is 7% in running velocity of 385 m/s. The above mentioned speed is very high and no high speed train reach to this right now. In the practical velocity range (less than 150 m/s), there are good correlation between the simulation model and the refereed paper.

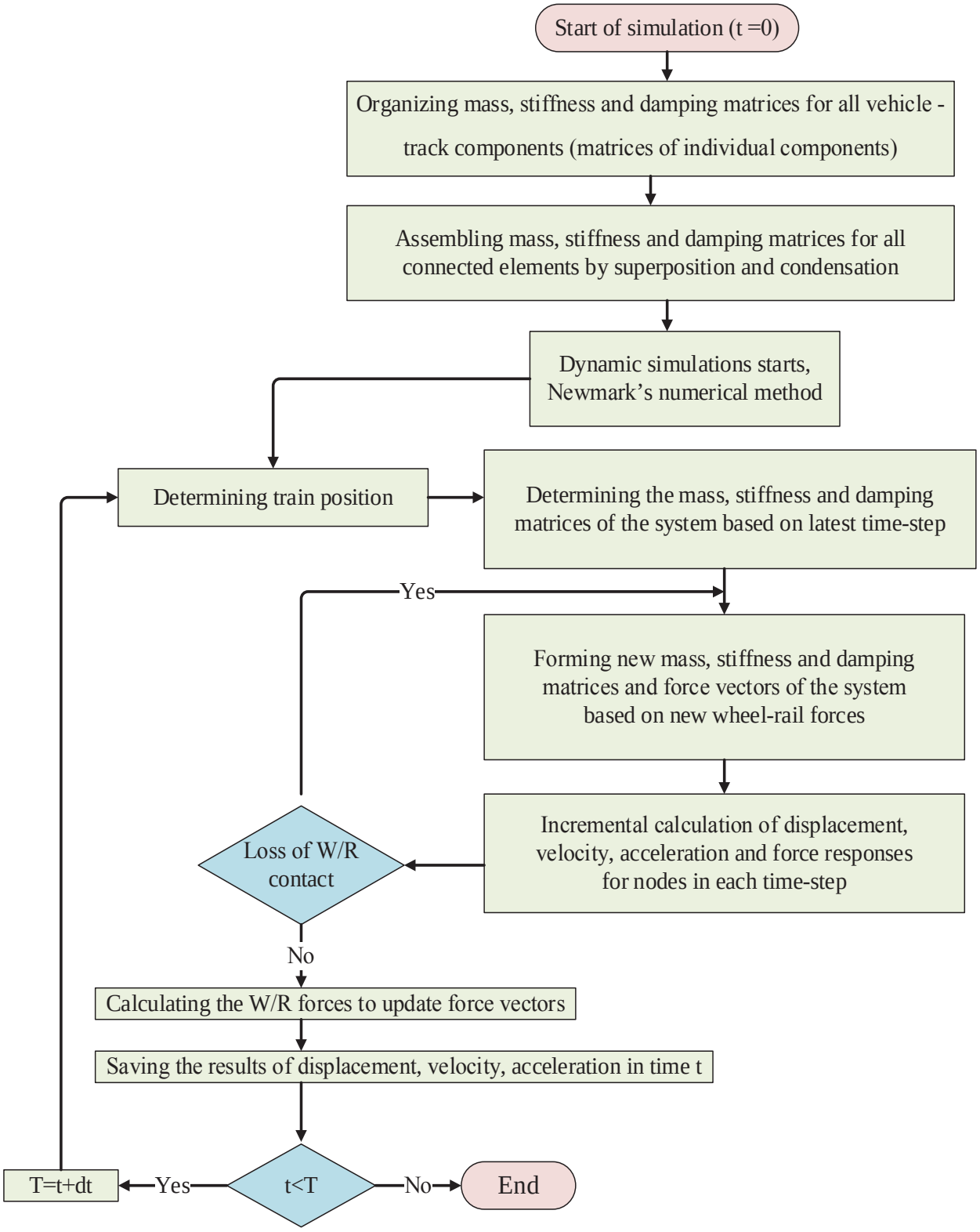

Figure 2. Flowchart of procedure of dynamic simulation of vehicle-FST

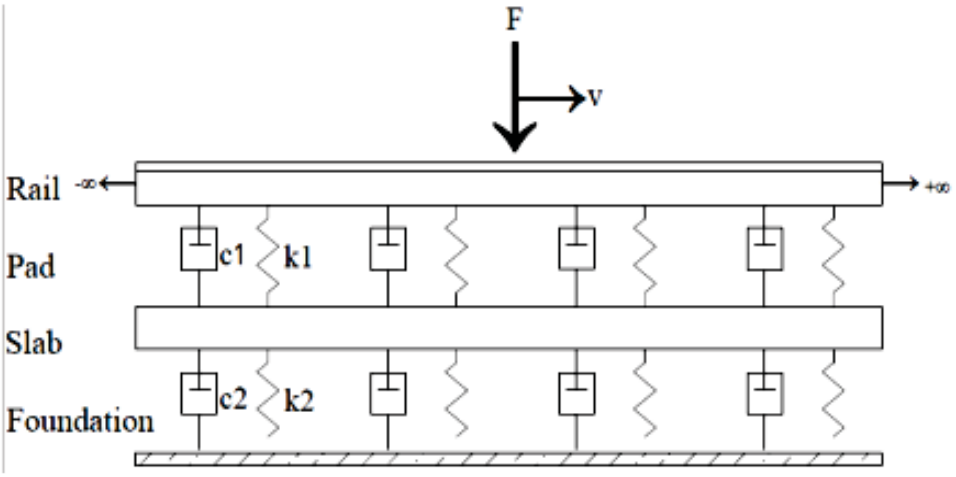

Figure 3. The simulation of double beam (FST)

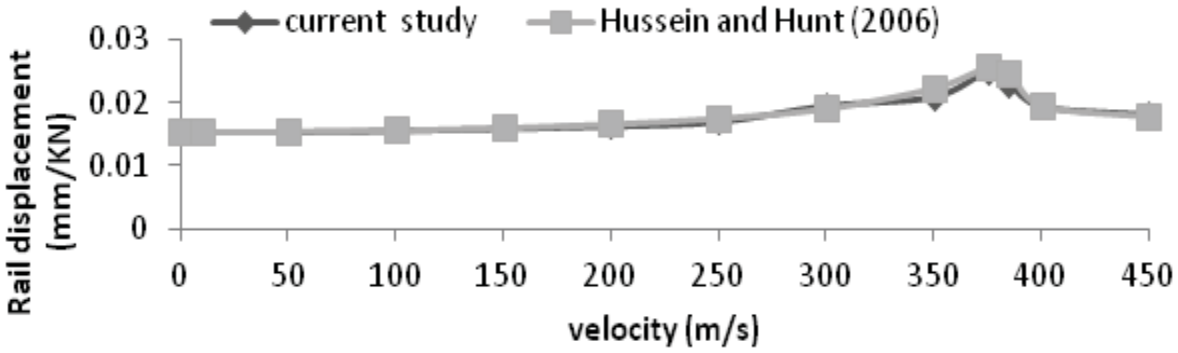

Figure 4. Comparing the results of FEM model and analytical model

Table 1. Comparison of the results of current FEM model with analytical model of [Hussein and Hunt, 2006]

velocity(m/s)	0	50	100	150	200	250	300	350	385	400	450	
Rail displacement (mm/KN)	Refereed	0.0155	0.0152	0.01573	0.0161	0.0167	0.0176	0.0192	0.022	0.025	0.0196	0.0179
	Simulated	0.0155	0.015	0.0157	0.016	0.0164	0.0171	0.0196	0.021	0.023	0.0195	0.0182
Difference (%)	0	0.13	0.2	0.69	1.8	3	2.3	6	7	0.7	1.6	

4.2 Sensitivi ty Analysis Results

This part of study is allocated to showing some various capabilities of the developed FE model in investigating the dynamic behaviour of slab track system under the moving vehicle.In this regard the vehicle move starts at the left-hand end of a 50 m long FST with a speed of 80 km/h and the steady state response of the coupled vehicle– FST system are obtained at the middle of the slab track. The selected length for analysis ensures that the end conditions do not influence the obtained results. The FST parameters are listed in Table 1.

In continue, many sensitivity analyses are performed to illustrate the effects of slab thickness, foundation stiffness, and axle load on dynamic behaviour of FST. The results will be presented in the form of rail and slab deflections and bending moments as well. Table 2 shows the parameters values which are used for sensitivity analyses in current study.

The thickness of slab affects directly on slab bending

stiffness. Figure 5 shows the deflection of the rail as a function of slab thickness. As illustrated, by increasing slab thickness, deflection of rail has negligible decreased.

Figure 6 shows the variation of rail deflection with slab thickness, foundation stiffness and axle load. Figure6.a shows that an increasing in the slab thickness, from 0.2 to 0.3 meter (k_2 equal to 50 MPa), would decrease of 0.36% in the rail deflection and an increasing of slab thickness from 0.2 to 0.4 meter would decrease of 0.72 % in the rail deflection. This effect in Fig5.b is equal to 0.38% and 0.76% and in Fig5.c is equal to 0.31% and 0.62%, respectively.

Table 2. Parameter values used for FST

Item	Notation	Value	Unit
(Rail (UIC 60			
Bending stiffness (steel)	E_1	$6.65*10^6$	pam^4
Mass per length	m_1	60.34	kgm^{-1}
Slab			
Bending stiffness (concrete)	E_2	$233.3*10^6$	pam^4
Mass per length	m_2	3500	kgm^{-1}
Rail pad			
Stiffness	k_1	$40*10^6$	Nm^{-2}
Viscous damping	c_1	$6.3*10^3$	$Ns\ m^{-2}$
Slab Bearing			
Viscous damping	c_2	$41.8*10^3$	$Ns\ m^{-2}$

Table 3. Parameter values used for sensitivity analysis of slab track

Item	Notation	Value	Unit
Slab thickness	d	0.2, 0.3, 0.4	m
Foundation stiffness	k_2	25, 50, 70, 110	MPa
Axle load	P	11,14.5,20	ton

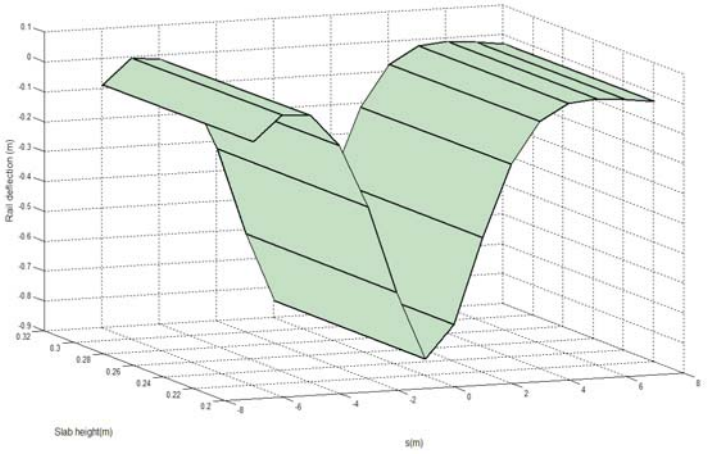

Figure 5. Variation of rail deflection with slab thickness, K_2 = 50 MPa, P=11 ton

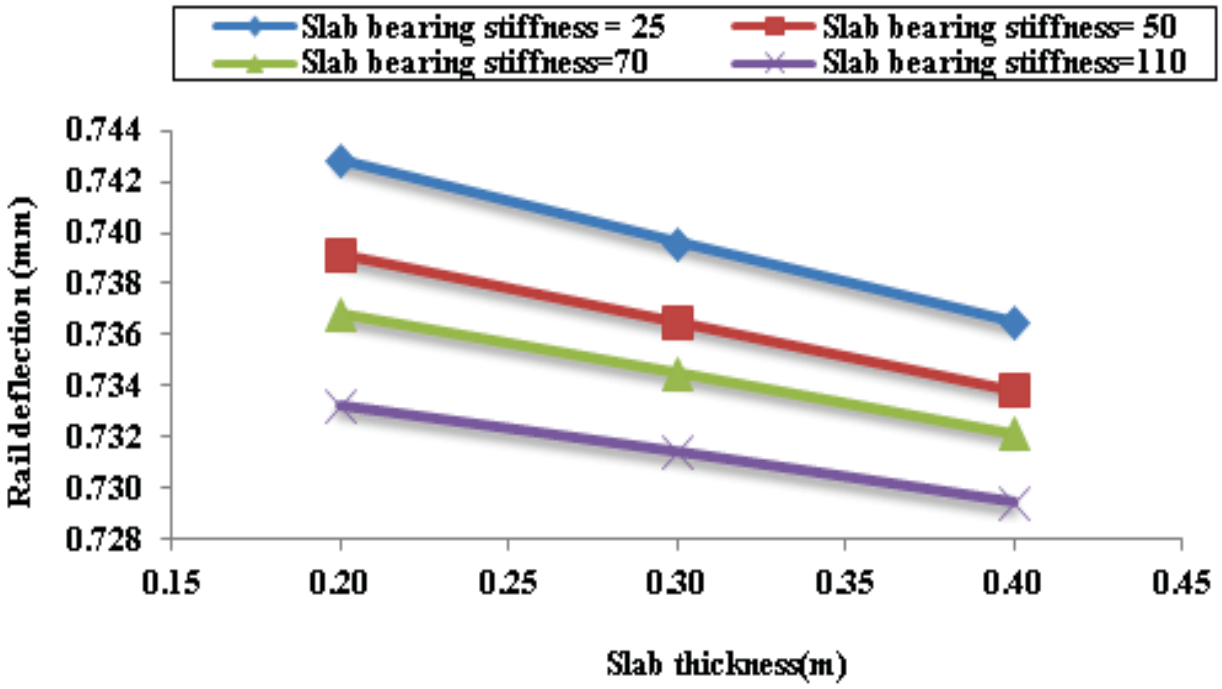
Slab bearing stiffness = 25
Slab bearing stiffness= 50
Slab bearing stiffness=70
Slab bearing stiffness=110
Rail deflection (mm)
0.744
0.742
0.740
0.738
0.736
0.734
0.732
0.730
0.728
0.15
0.20
0.25
0.30
0.35
0.40
0.45
Slab thickness(m)

(a)

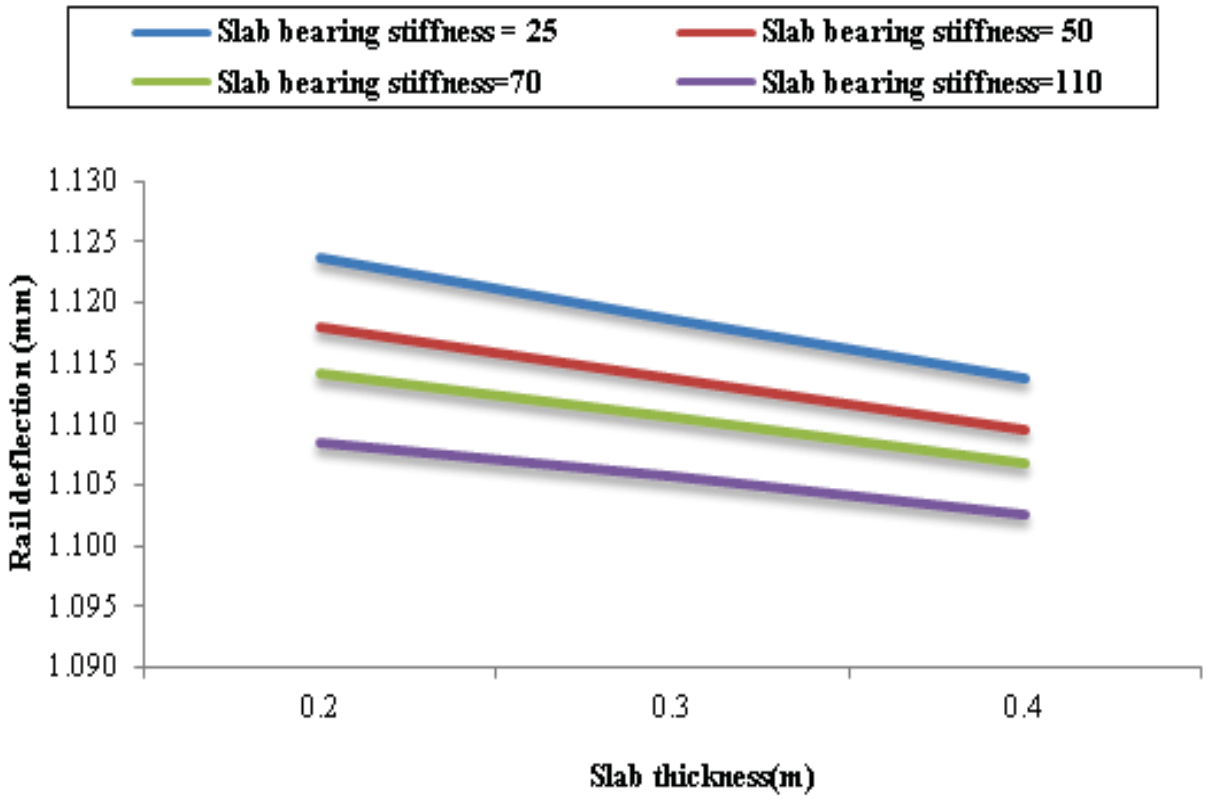
Slab bearing stiffness = 25
Slab bearing stiffness= 50
Slab bearing stiffness=70
Slab bearing stiffness=110
Rail deflection (mm)
1.130
1.125
1.120
1.115
1.110
1.105
1.100
1.095
1.090
0.2
0.3
0.4
Slab thickness(m)

(b)

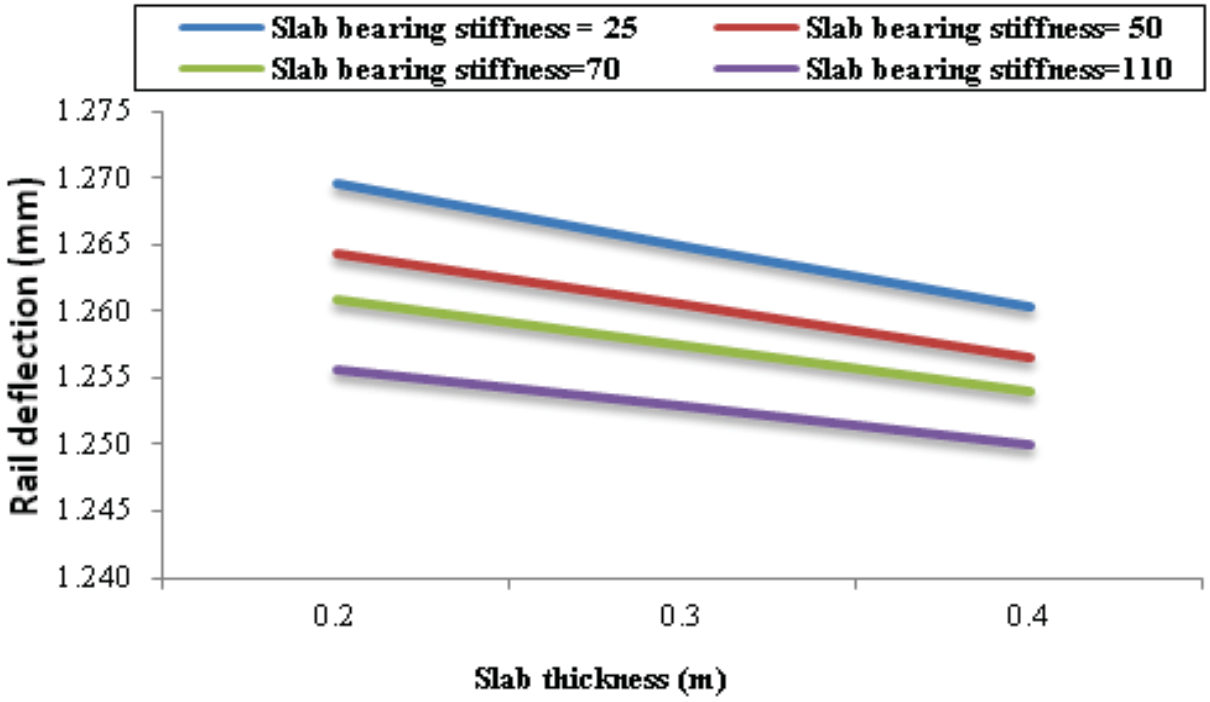

(c)

Figure 6. Variation of rail deflection versus slab thickness, (a) axle load=11 ton (b) axle load=14.5 ton (c) axle load=20 ton

An increase in slab foundation stiffness from 25 to 50 Mpa (slab thickness and axle load equal to 0.2 m and 11 ton, respectively) can cause a decrease of 0.5% in the rail deflection and an increase of slab foundation stiffness from 25 to 70 MPa and 25 to 110 MPa would decrease the rail deflection by 0.8 % and 1.3%, respectively.

The effect of value of axle load which is moving along the rail is illustrated in Figs .6(a) - (c). The amplitude of the load is considered vary as 10, 14.5 and 20 ton. Sensitivity analysis results on the axle load shows that increasing in the axle load from 10 to 14.5 ton (k_2 equal to 50 MPa and slab thickness equal to 0.2 m) increases the rail deflection by 34%. Also an increasing of axle load from 10 to 20 ton can cause an increase of 41.5 % in the rail deflection. Figure 7 shows the variation of rail deflection with axle load in the middle of the rail.

Figure 8 shows the variation of rail bending moment versus slab thickness. As it shown, by increasing the slab thickness, rail bending is reduced (for constant slab foundation stiffness). In other hand, by increasing the K_2 ,the rail bending moment is increased (while the slab thickness is increased).

As shown in Figure 9, by increasing the slab thickness, the defelction of slab is decreased. Figure9.a shows that an increase in slab thickness, from 0.2 to 0.3 meter (assuming the k_2 equal to 50 MPa), can decrease the slab deflection by 13.7% and an the increase in slab thickness from 0.2 to 0.4 meter can decreases the slab deflection by 25.7 %. The above variations about slab thickness were calculated for 14.5 ton axle load (Fig 9.b) and 20 ton axle load (Fig 9.c). So, the variation is equal to 13.72% and 25.7% and 13.6% and 25.5%, respectively.

An increase in slab foundation stiffness from 25 to 50 Mpa (assuming the slab thickness and axle load equal to 0.2 m and 11 ton, respectively) would cause a decrease of 11% in the slab deflection and an increase of slab foundation stiffness from 25 to 70 MPa and 25 to 110 MPa would produce a decrease of 19 % and 30% in the slab deflection, respectively.

The effect of value of axle load which is moving along

the rail is illustrated in Figs. 9(a)-(c). The amplitude of the load is considered to be 10, 14.5 and 20 ton. Sensitivity analysis on the axle load shows that an increasing in the axle load, from 10 to 14.5 ton (assuming the k_2 equal to 50 MPa and slab thickness equal to 0.2 m) would cause an increase of 34% in the slab deflection. Also increasing of axle load from 10 to 20 ton would increase the slab deflection by 41 %.

Slab bending moment is one of the most important parameters in slab track design. Figure 10 represents the variation of this parameter versus slab thickness, slab foundation stiffness and axle load. By increasing the slab thickness, the bending moment of slab is increased. Indeed, increasing the slab foundation stiffness decreases the slab bending moment. It is obvious that by increasing the axle load, the slab bending moment is increased.

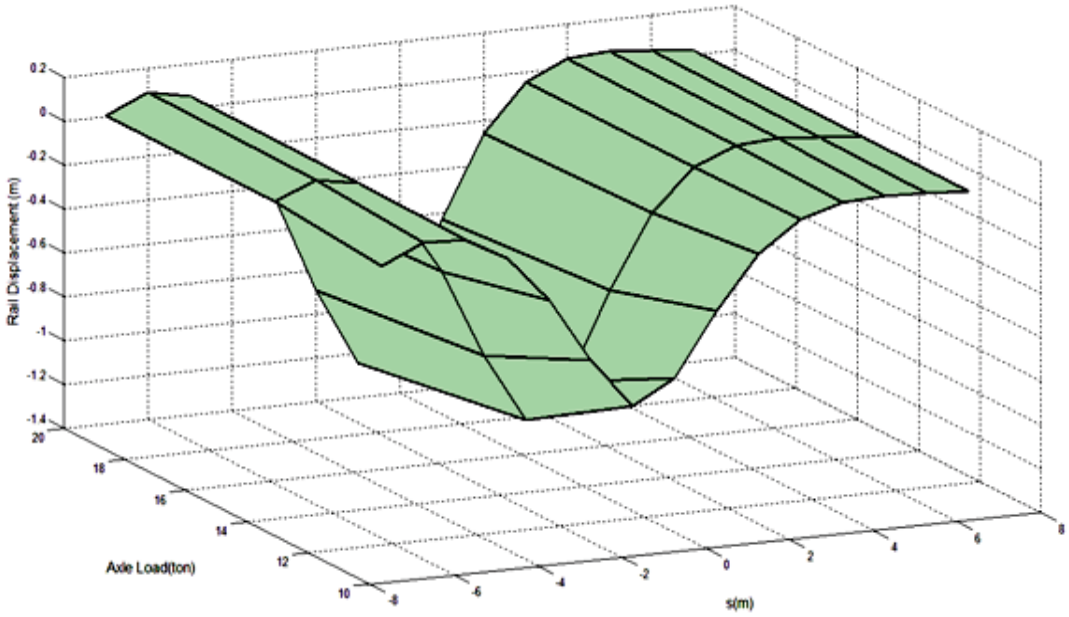

Figure 7. Variation of rail displacement with axle load, d=0.2 m, k2=50 MPa

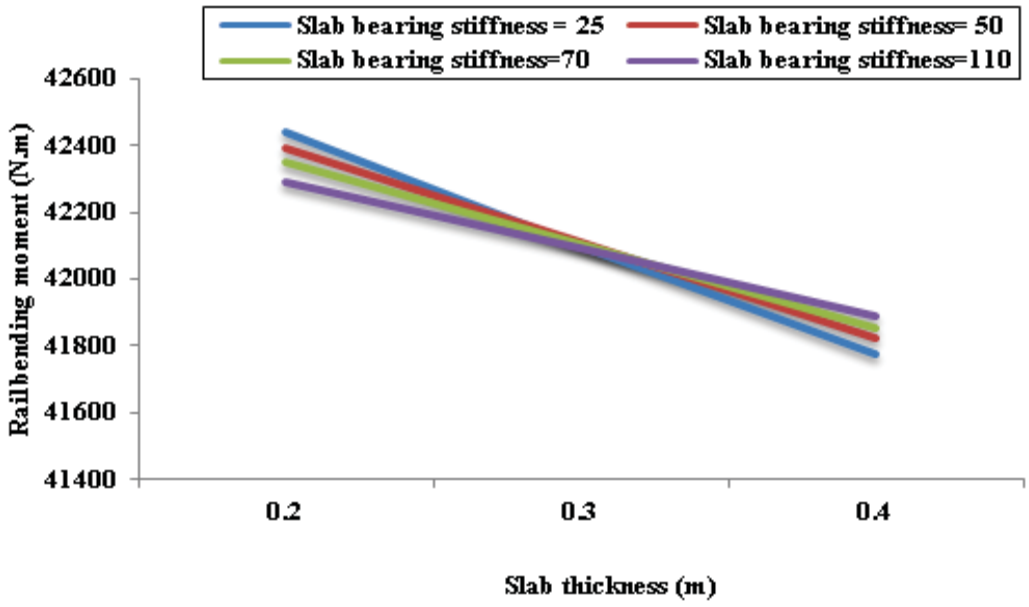

(a)

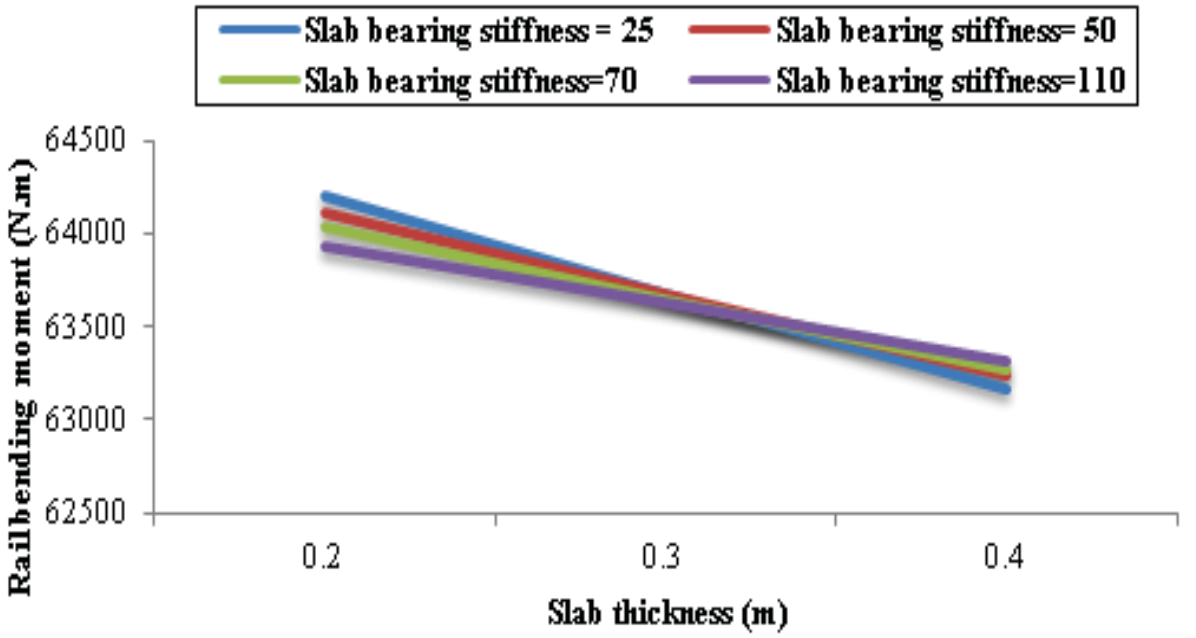

(b)

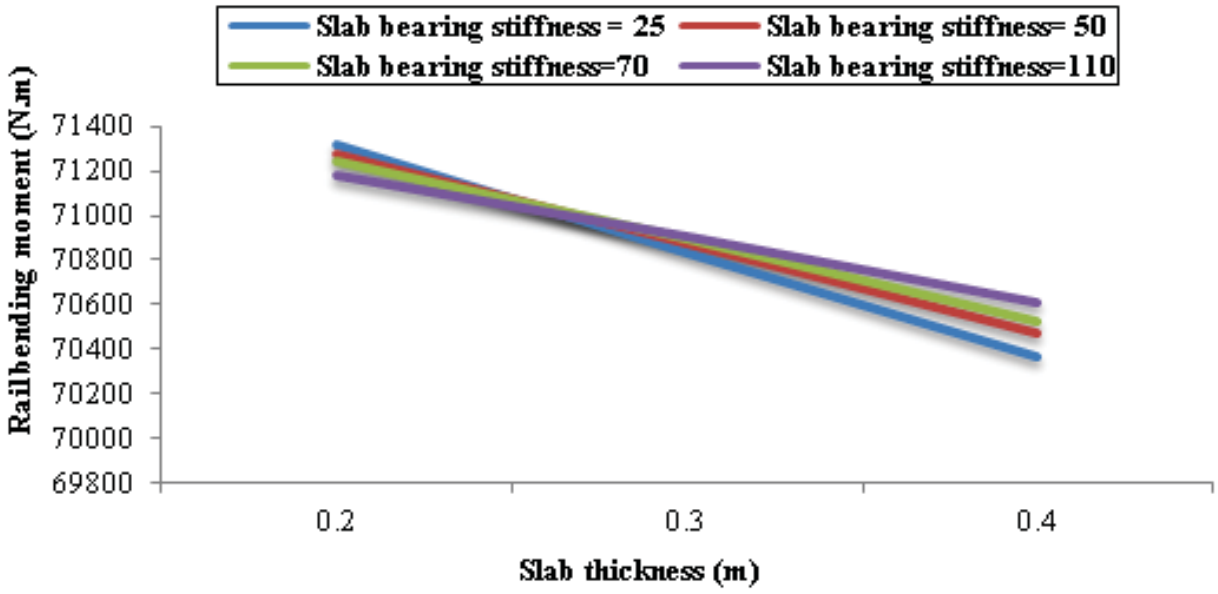

(c)

Figure 8. Variation of rail bending moment with slab thickness for (a) axle load=11 ton (b) axle load=14.5 ton (c) axle load=20 ton

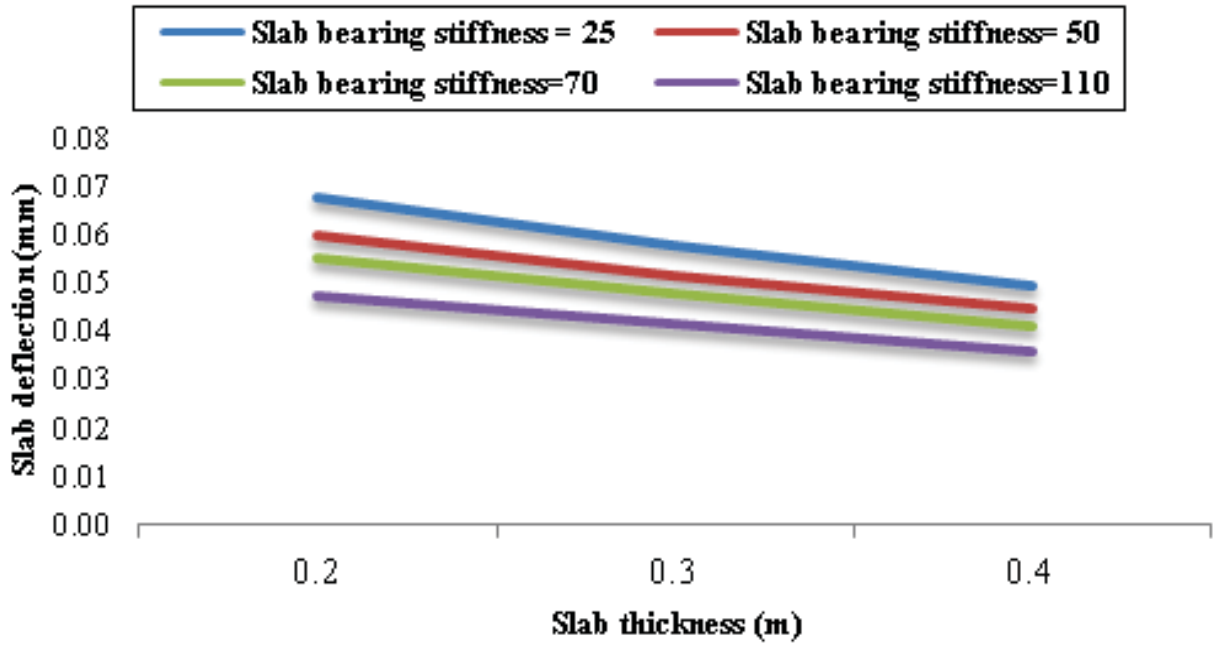
Slab bearing stiffness = 25
Slab bearing stiffness= 50
Slab bearing stiffness=70
Slab bearing stiffness=110
Slab deflection (mm)
0.08
0.07
0.06
0.05
0.04
0.03
0.02
0.01
0.00
0.2
0.3
0.4
Slab thickness (m)

(a)

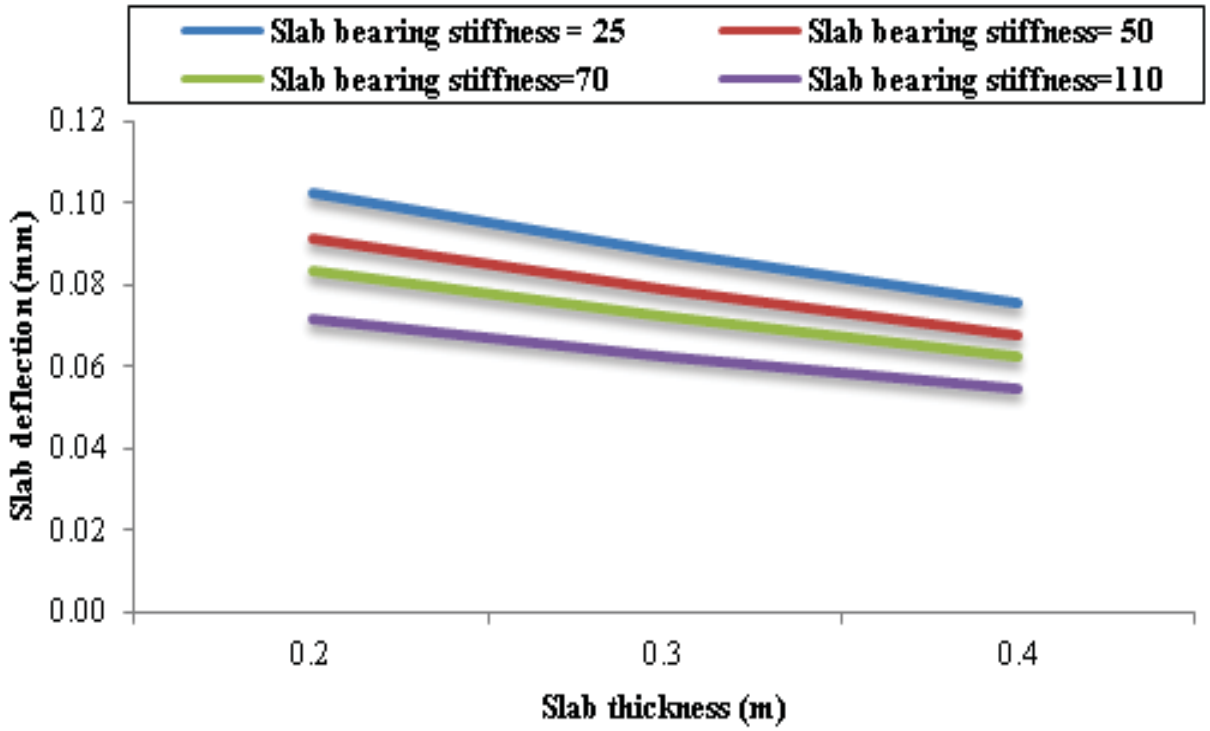
Slab bearing stiffness = 25
Slab bearing stiffness= 50
Slab bearing stiffness=70
Slab bearing stiffness=110
Slab deflection (mm)
0.12
0.10
0.08
0.06
0.04
0.02
0.00
0.2
0.3
0.4
Slab thickness (m)

(b)

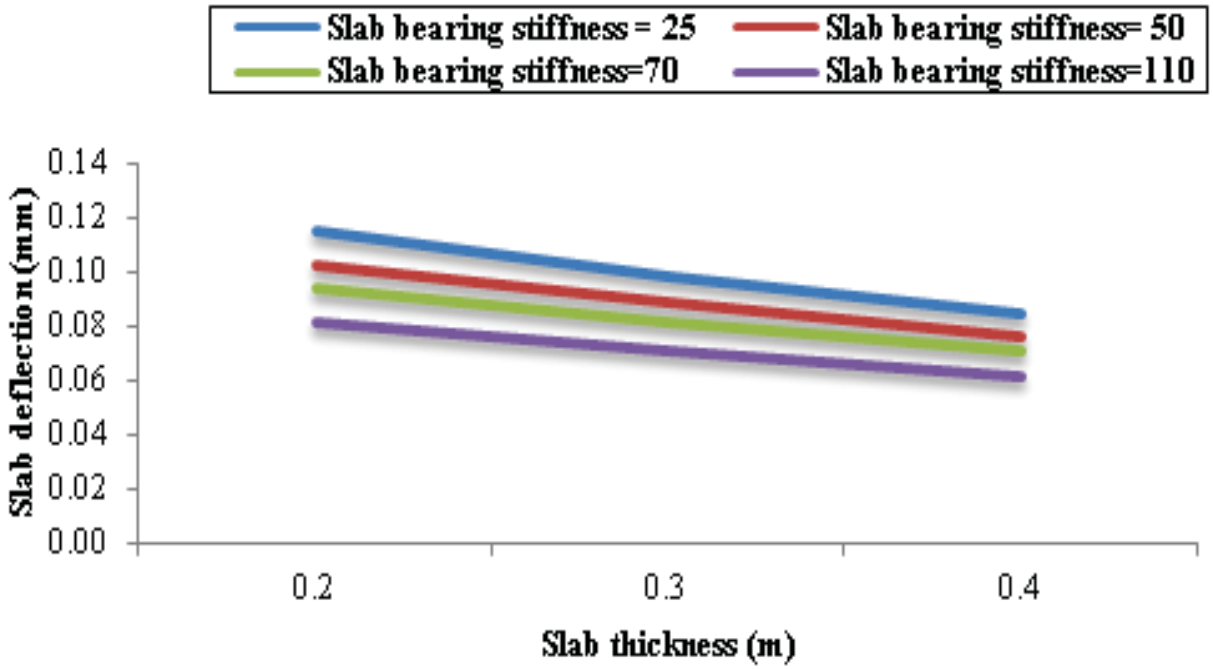

(C)

Figure 9. Variation of slab deflection with slab thickness for (a) axle load=11 ton(b) axle load=14.5 ton (c) axle load=20 ton

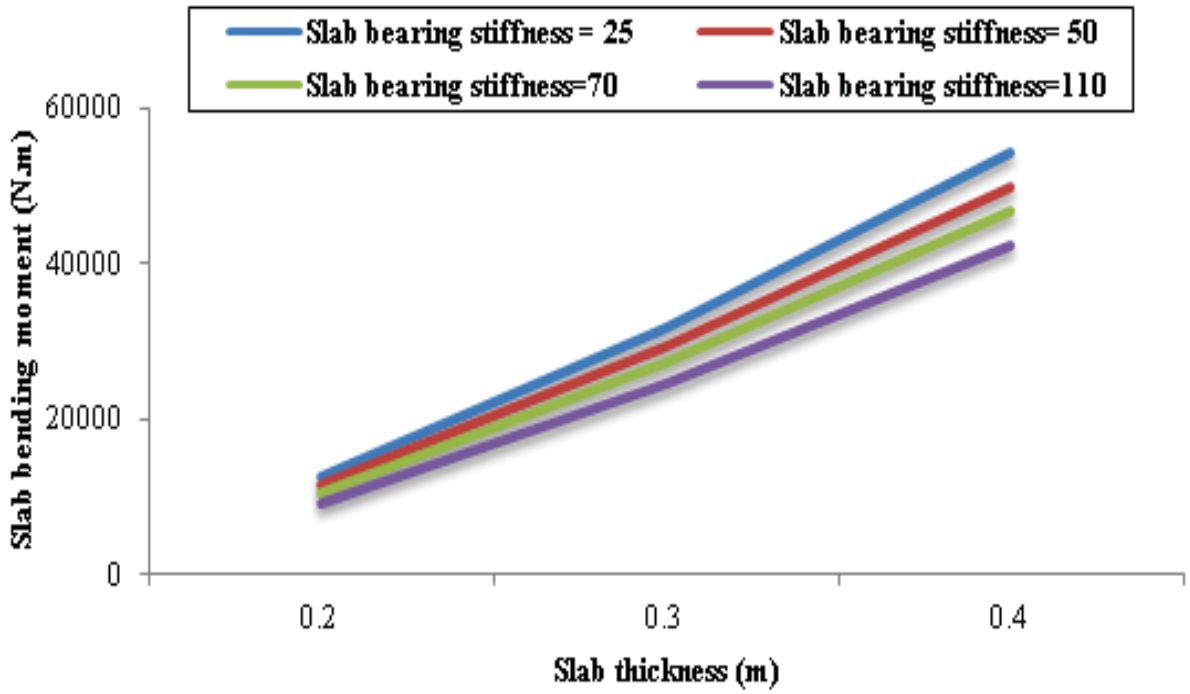

(a)

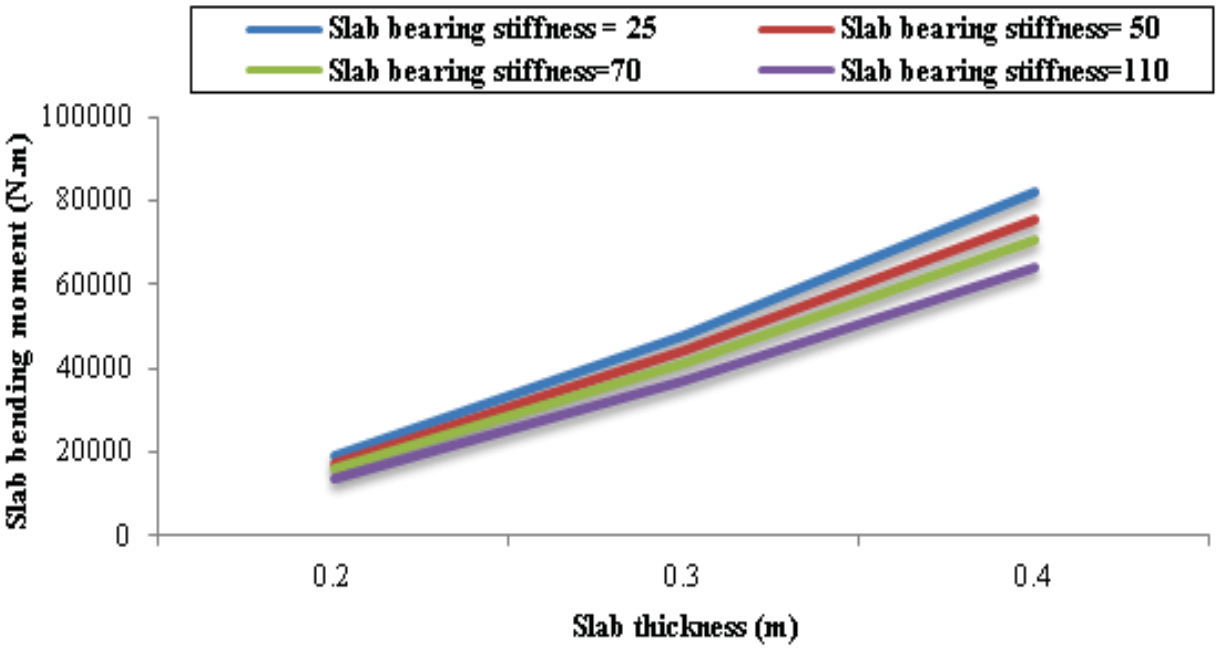

(b)

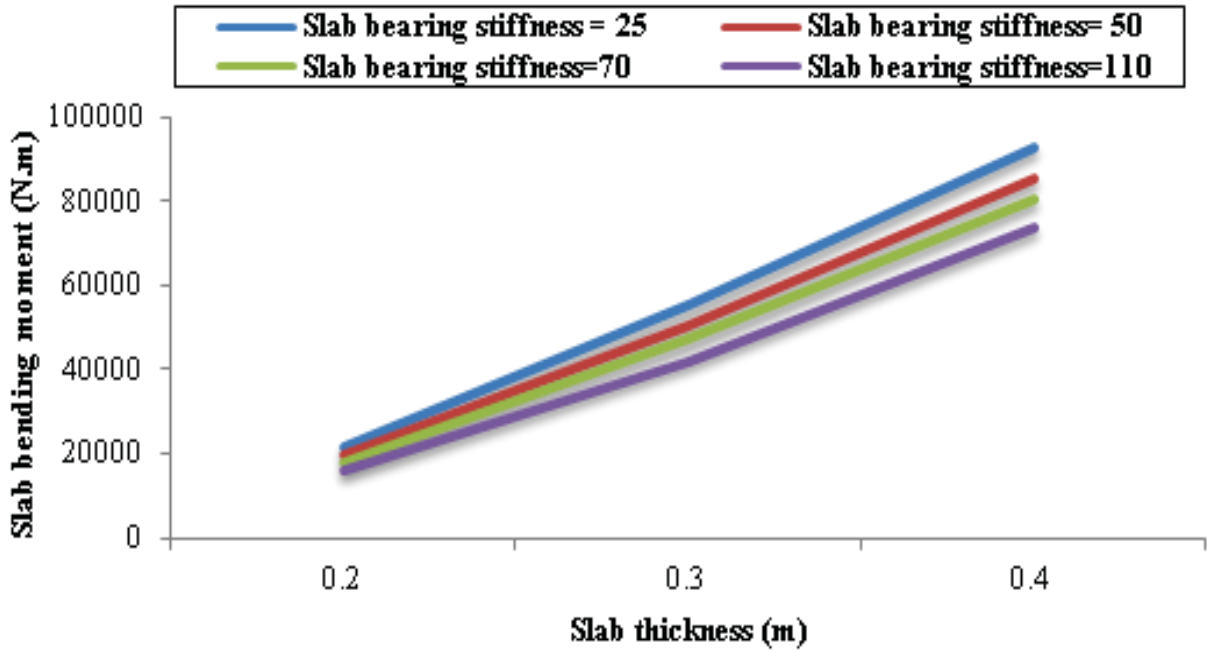

(c)

Figure 10. Variation of slab bending moment with slab thickness, (a) axle load=11 ton (b) axle load=14.5 ton (c) axle load=20 ton

5. Conclusion

The dynamic behaviour of slab track has been investigated by finite element method. The track has modelled by double beam theory. The rail and slab have been modelled by Euler-Bernoulli beam formulation. The rail pads and track bed have also been simulated with springs and dashpots. The loading condition has introduced by a moving wagon which it has been modelled by FEM including ten degree of freedom. Consequently, the effect of technical and operational parameters on slab track behaviour has been investigated by extensive sensitivity analyses. The main findings of the research can be presented as follows:

- An increase in the slab thickness, from 0.2 to 0.3 meter (assuming k_2 equal to 50 MPa and axle load equal to 11 ton), would cause a decrease of 0.36% in the rail deflection while increasing of slab thickness from 0.2 to 0.4 meter would decrease the rail deflection by 0.72 %. These values respectively change to 13.7% and 25.7% in the case of slab deflection.
- Increase in axle load, from 10 to 14.5 ton (supposing k_2 equal to 50 MPa and slab thickness equal to 0.2 m) cause an increase of 34% in the rail deflection. Also the increasing of axle load from 10 to 20 ton would produce an increase of 41.5 % in the rail deflection. These values respectively change to 34% and 41% for slab deflection.
- Rail bending moment decreases due to increase in slab thickness, but by increasing the slab foundation stiffness the rail bending moment increases by increase in slab thickness.
- Overall, by increasing the slab thickness, its bending moment increases.

6. References

-Abu-Hilal, M. (2006) "Dynamic response of a double Euler–Bernoulli beam due to a moving constant load", Journal of Sound and Vibration, Vol. 297, pp.477–491.

-Ames, W. F., Ames, W. (1972) "Nonlinear partial differential equations in engineering", vol. 2. Academic Press, New York (1972).

-Chen, Y. H. and Shiu Z. M. (2004) "Resonant curves of an elevated railway to harmonic moving loads", International Journal of Structural Stability and Dynamics, Vol. 4, No.2, pp. 237–257.

-Cox, S. J, Wang, A., Morison, C., Carels, P., Kelly, R. and Bewes, O. G. (2006) "A test rig to investigate slab track structures for controlling ground vibration", Journal of Sound and Vibration, Vol. 293, pp. 901–909.

-Ding, D-y, Liu, W-n, Li, K-f, Sun, X-J. and Liu, W-f. (2011) "Low frequency vibration tests on a floating slab track in an underground laboratory", Journal of Zhejiang University-Science A (Applied Physics & Engineering), Vol.12, No.5, pp.345-359.

-Gupta, S. and Degrande, G. (2009) "Modelling of continuous and discontinuous floating slab tracks in a tunnel using a periodic approach", Journal of Sound and Vibration, Vol. 329, pp. 1101–1125.

-Hussein, M. F. M. and Hunt, H. E. M. (2006) "Modelling of floating-slab tracks with continuous slabs under oscillating moving loads", Journal of Sound and Vibration, Vol. 297, pp. 37–54.

-Hussein, M. F .M. and Hunt, H.E.M. (2009) "A numerical model for calculating vibration due to a harmonic moving load on a floating-slab track with discontinuous slabs in an underground railway tunnel", Journal of Sound and Vibration, Vol. 297, pp. 901–909.

-Jun, X. , Dan, H. and Qing-yuan, Z. (2008) "Analysis theory of spatial vibration of high-speed train and slab track system", Journal of Central South University of Technology, Vol.15, pp.121-126.

-Kalker, J. J. (1991) "Wheel rail rolling contact theory". Wear, 144, pp.243–261.

-Kuo, Chen-Ming, Huang, Cheng-Hao and Chen, Yi-Yi (2008) "Vibration characteristics of floating slab track", Journal of Sound and Vibration, Vol.317, pp. 1017–1034.

-Li, Z. G. and Wu T. X. (2008) "Modelling and analy-

sis of force transmission in floating-slab track for railways", Journal of Rail and Rapid Transit, Part F, Vol. 222, pp.45-57.

-Lombaert, G., Degrande, G., Vanhauwere, B., Vandeborght, S. and Francois, S. (2006) "The control of ground-borne vibrations from railway traffic by means of continuous floating slabs", Journal of Sound and Vibration, Vol. 297, pp.363–374.

-Mehrali, M., Mohammadzadeh, S., Esmaeili, M. and Nouri, M. (2014) "Investigating vehicle-slab track interaction considering random track bed stiffness", Scientia Iranica, Transactions A: Civil Engineering, Vol. 21, pp. 82-90.

-Mohammadzadeh, S., Esmaeili, M. and Mehrali, M. (2013) "Dynamic response of double beam rested on stochastic foundation under harmonic moving load", International Journal for Numerical and Analytical Methods in Geomechanics, doi: 10.1002/nag.2227.

-Mohammadzadeh, S., Ahadi, S. and Keshavarzian, H. (2014) "Assessment of fracture reliability analysis of crack growth in spring clip type Vossloh SKL14. Proc. Inst. Mech. Eng. O: J. Risk Reliab.

-Saurenman, H., Phillips, J. (2006) "In-service tests of the effectiveness of vibration control measures on the BART rail transit system", Journal of Sound and Vibration, Vol. 293, pp.888–900.

-Steenbergen, M.J.M.M., Metrikine, A.V. and Esveld, C. (2007) "Assessment of design parameters of a slab track railway system from a dynamic viewpoint", Journal of Sound and Vibration, Vol. 306, pp. 361-371.

-Xiaobin, L., Shuangxi, X., Weiguo, Wu., Jun, L. (2014) "An exact dynamic stiffness matrix for axially loaded double-beam systems", Sadhana, Vol. 39 No.3, pp. 607-623.

-Yen, S. T. and Lee, Y.H. (2007) "Parameter identification and analysis of a slab track system using 3d ABAQUS program", Journal of Transportation Engineering © ASCE, pp. 288-297.

-Yuan, J., Zhu, Y. and Wu, M. (2009) "Vibration characteristics and effectiveness of floating slab track system", Journal of Computers, Vol.4, No.12, pp. 1249-1254.

-Zakeri, J. A. and Xia, H. (2008) "Sensitivity analysis of track parameters on train- track dynamic interaction", Journal of Mechanical Science and Technology, Vol.22, No.7, pp. 1299-1304.

-Zhai,W., Wang, K. and Cai, C. (2009) "Fundamental of vehicle-track coupled dynamic", Journal of vehicle system dynamics, Vol.47, No. 11, pp. 1349-1376.

-Zhao, X., Li Z. (2011) "The solution of frictional wheel–rail rolling contact with a 3D transient finite element model: validation and error analysis". Wear, Vol. 271, pp.444–452.

-Zhao, X., Li, Z. and Liu, J. (2012) "Wheel–rail impact and the dynamic forces at discrete supports of rails in the presence of singular rail surface defects", Proceeding of the Institution of Mechanical Engineering, Part F Journal of Rail and Rapid Transit, Vol.226, pp.124–139.

APPENDIX

In the following, the equation motions of vehicle are listed:

Carbody	Vertical	$M_c\ddot{Z}_c + K_s(Z_c - Z_{t1}) + K_s(Z_c - Z_{t2}) + C_s(\dot{Z}_c - \dot{Z}_{t1}) + C_s(\dot{Z}_c - \dot{Z}_{t2}) = 0$
	yawing	$J_c\ddot{\psi}_c + K_s l_c(l_c\psi_c - Z_{t1}) + K_s l_c(l_c\psi_c + Z_{t2}) + C_s l_c(l_c\dot{\psi}_c - \dot{Z}_{t1}) + C_s l_c(l_c\dot{\psi}_c + \dot{Z}_{t2}) = 0$
First bogie	Vertical	$M_t\ddot{Z}_{t1} + K_t(Z_{t1} - Z_c - \psi_c l_c) + K_w(Z_{t1} - Z_{w1}) + K_w(Z_{t1} - Z_{w2}) + C_t(\dot{Z}_{t1} - \dot{Z}_c - \dot{\psi}_c l_c) + C_w(\dot{Z}_{t1} - \dot{Z}_{w1}) + C_w(\dot{Z}_{t1} - \dot{Z}_{w2}) = 0$
	yawing	$J_t\ddot{\psi}_{t1} + K_p l_t(l_t\psi_{t1} - Z_{w1}) + K_p l_t(l_t\psi_{t1} + Z_{w2}) + C_p l_t(l_t\dot{\psi}_{t1} - \dot{Z}_{w1}) + C_p l_t(l_t\dot{\psi}_{t1} + \dot{Z}_{w2}) = 0$
Second bogie	Vertical	$M_t\ddot{Z}_{t2} + K_s(Z_{t2} - Z_c + \psi_c l_c) + K_p(Z_{t2} - Z_{w3}) + K_p(Z_{t2} - Z_{w4}) + C_s(\dot{Z}_{t2} - \dot{Z}_c - \dot{\psi}_c l_c) + C_p(\dot{Z}_{t2} - \dot{Z}_{w3}) + C_p(\dot{Z}_{t2} - \dot{Z}_{w4}) = 0$
	yawing	$J_t\ddot{\psi}_{t2} + K_p l_t(l_t\psi_{t2} - Z_{w3}) + K_p l_t(l_t\psi_{t2} + Z_{w4}) + C_p l_t(l_t\dot{\psi}_{t2} - \dot{Z}_{w3}) + C_p l_t(l_t\dot{\psi}_{t2} + \dot{Z}_{w4}) = 0$
1st Wheel	Vertical	$M_w\ddot{Z}_{w1} + K_p(Z_{w1} - Z_{t1} - l_t\psi_{t1}) + C_p(\dot{Z}_{w1} - \dot{Z}_{t1} - l_t\dot{\psi}_{t1}) + F_{w1}(t) = 0$
2st Wheel		$M_w\ddot{Z}_{w2} + K_p(Z_{w2} - Z_{t1} + l_t\psi_{t1}) + C_p(\dot{Z}_{w2} - \dot{Z}_{t1} + l_t\dot{\psi}_{t1}) + F_{w2}(t) = 0$
3st Wheel		$M_w\ddot{Z}_{w3} + K_p(Z_{w3} - Z_{t2} - l_t\psi_{t2}) + C_p(\dot{Z}_{w3} - \dot{Z}_{t2} - l_t\dot{\psi}_{t2}) + F_{w3}(t) = 0$
4st Wheel		$M_w\ddot{Z}_{w4} + K_p(Z_{w4} - Z_{t2} + l_t\psi_{t2}) + C_p(\dot{Z}_{w4} - \dot{Z}_{t2} + l_t\dot{\psi}_{t2}) + F_{w4}(t) = 0$